Contrasting short-term plasticity at two sides of the mitral–granule reciprocal synapse in the mammalian olfactory bulb

Shelby B. Dietz[1] and Venkatesh N. Murthy[2]

[1] *Graduate Program in Neuroscience, Harvard Medical School, Boston, MA, USA*
[2] *Department of Molecular and Cellular Biology, Harvard University, Cambridge, MA, USA*

The mitral–granule reciprocal synapse shapes the response of the olfactory bulb to odour stimuli by mediating lateral and reciprocal inhibition. We investigated the short-term plasticity of both the mitral-to-granule excitatory synapse and the granule-to-mitral inhibitory synapse in rat olfactory bulb slices, using whole-cell patch clamp recordings. The granule-to-mitral inhibitory synapse invariably exhibited paired-pulse depression at interstimulus intervals of less than a second, while the mitral-to-granule excitatory synapse showed heterogeneous responses, which on average yielded a moderate facilitation. Trains of stimuli led to a much greater depression at the granule-to-mitral synapse than at the mitral-to-granule synapse. Since mitral cells commonly respond to odours by burst firing with each inhalation cycle, we used bursts of stimuli to study recovery from depression. We found that recovery from depression induced by fast trains of stimuli was more rapid at the mitral-to-granule synapse than at the granule-to-mitral synapse. In addition, depression was enhanced by higher calcium concentrations, suggesting at least partial contribution of presynaptic mechanisms to short-term depression. The observed short-term plasticity could enable mitral cells to overcome autoinhibition and increase action potential propagation along lateral dendrites by burst firing.

(Resubmitted 2 August 2005; accepted after revision 13 September 2005; first published online 15 September 2005)
Corresponding author V. N. Murthy: Department of Molecular and Cellular Biology, Harvard University, 16 Divinity Avenue, Cambridge, MA 02138, USA. Email: vnmurthy@fas.harvard.edu

Mitral and tufted cells are the principal excitatory cells of the olfactory bulb (Shepherd & Greer, 1998; Mori *et al.* 1999; Schoppa & Urban, 2003). They receive input from the olfactory receptor neurones in the nares and project their axons to the olfactory cortex and other higher brain regions. Because of their position at an anatomical bottleneck, mitral and tufted cells are presumed to carry, through their firing patterns, all odour information between the nose and brain.

Odour information carried by olfactory receptor axons is transformed and processed by local circuits within the olfactory bulb. In particular, GABAergic inhibition is thought to play an important role in shaping mitral cell firing patterns. A mitral cell *in vivo* can respond to an odour with a wide variety of firing patterns, including increasing or decreasing its basal firing rate (Meredith, 1986; Hamilton & Kauer, 1989; Imamura *et al.* 1992; Yokoi *et al.* 1995; Kashiwadani *et al.* 1999; Wilson, 2000; Luo & Katz, 2001; Margrie *et al.* 2001; Cang & Isaacson, 2003). The firing rate of a mitral cell that is excited by an odour frequently adapts to sensory input (Wilson, 2000; Margrie *et al.* 2001). Application of the $GABA_A$ receptor antagonist bicuculline to the mitral cell layer increases excitatory mitral cell responses to odours, and decreases inhibitory responses (Yokoi *et al.* 1995). Bicuculline also blocks the adaptation of mitral cell firing rate, indicating that GABAergic currents are critical for this accommodation (Margrie *et al.* 2001). Application of bicuculline to the antennal lobes, the insect equivalent of the mammalian olfactory bulb, disrupts the animal's ability to distinguish between similar odours (Stopfer *et al.* 1997).

The mitral–granule reciprocal synapse has been regarded as the most likely synapse through which lateral inhibition is mediated, because it provides a lateral connection between putative glomerular 'odour columns' (DeVries & Baylor, 1993; Shepherd & Greer, 1998), although recent studies have pointed out an additional source of lateral inhibition in the glomerular layer (Aungst *et al.* 2003). In the mitral–granule lateral inhibitory circuit, granule cells form dendrodendritic reciprocal synapses on mitral cell lateral dendrites. Mitral cell lateral dendrites can span several hundred micrometres, presumably sampling

 DOI: 10.1113/jphysiol.2005.095844

granule cells that receive excitatory inputs from other mitral cells projecting to different glomeruli (Shepherd & Greer, 1998).

In addition to providing lateral inhibition, the reciprocal synapses between mitral and granule cells also generate autoinhibition of mitral cells (Rall *et al.* 1966; Nicoll, 1969; Jahr & Nicoll, 1982; Isaacson & Strowbridge, 1998; Schoppa *et al.* 1998). This dendrodendritic inhibition (DDI) has been studied in detail in recent years, largely using strong depolarizing pulses in mitral cells that generate feedback inhibition in the form of a barrage of IPSCs (Chen & Shepherd, 1997; Isaacson & Strowbridge, 1998; Friedman & Strowbridge, 2000; Margrie *et al.* 2001). The extent of DDI, as measured as the bicuculline-sensitive IPSP following a burst of mitral cell action potentials, is directly correlated with the number of action potentials in the burst, both *in vivo* and *in vitro* (Margrie *et al.* 2001). GABA release onto lateral dendrites, evoked by either stimulation of granule cells (Halabisky & Strowbridge, 2003) or direct uncaging of GABA (Lowe, 2002), reduces mitral cell firing in response to current injection. Plasticity in the extent of inhibition from burst to burst of mitral cell activity should therefore have a profound impact on the evolving mitral cell response over the course of an odour presentation.

To understand how the mitral–granule reciprocal synapse could shape a mitral cell's firing rate over the time course of odour exposure, we must characterize the synapse's short-term plasticity. Facilitation and depression, both present in varying degrees in most synapses, combine to modulate synaptic strength during patterns of stimulation (Tsodyks & Markram, 1997; Abbott *et al.* 1997; Dittman *et al.* 2000; Cook *et al.* 2003). In this paper, we show that the mitral-to-granule and granule-to-mitral sides of the reciprocal synapse display very different patterns of short-term facilitation and depression, which could have significant consequences for mitral cell firing patterns during sustained or repetitive olfactory stimulation.

Methods

Slice preparation

Rats aged P9–17 were sedated with CO_2 and decapitated. Their skulls were quickly removed and their olfactory bulbs, along with the anterior forebrain, submerged in ice-cold, filtered, oxygenated choline chloride solution (mM: 110 choline chloride, 25 $NaHCO_3$, 25 glucose, 2.5 KCl, 1.25 NaH_2PO_4, 0.5 $CaCl_2$, 7 $MgCl_2$, 11.6 sodium ascorbate, 3.1 sodium pyruvate, pH 7.3, osmolality 290–300 mosmol kg^{-1}). The dura were removed and the bulbs and anterior forebrain glued onto the stage of a Pelco series 1000 vibratome (Ted Pella, Inc., Redding, CA, USA) or a Leica VT1000S vibratome (Leica Microsystems, Nussloch, Germany), while being perfused with choline chloride continually bubbled with 95/5 O_2/CO_2. Horizontal slices of 300 μm were cut and removed to oxygenated, buffered saline (mM: 119 NaCl, 26.2 $NaHCO_3$, 11 glucose, 2.5 KCl, 1 NaH_2PO_4, 2.5 $CaCl_2$, 1.5 $MgCl_2$, pH 7.3, osmolality 290–300 mosmol kg^{-1}) at 35°C. The slices were initially incubated at 35°C, and then cooled to room temperature over 45–60 min before being stored at room temperature. Animal care and experimental procedures adhered to guidelines approved by the Harvard University IACUC and conformed to NIH guidelines.

Recordings

Slices were visualized using an Olympus BX50WI upright microscope equipped with DIC optics and a 60× water immersion objective, and whole-cell voltage clamp recordings were made using an Axopatch 200B amplifier (Axon Instruments, Union City, CA, USA). Currents were filtered at 2 kHz and sampled at 10 kHz using custom acquisition software written in MATLAB (The MathWorks, Natick, MA, USA), Microsoft Visual Basic (Microsoft, Redmond, WA, USA), and IGOR Pro (WaveMetrics, Lake Oswego, OR, USA). An A-M Systems model 2100 isolated pulse stimulator (A-M Systems, Carlsborg, WA, USA) connected to a monopolar glass microelectrode was used for extracellular stimulation. Mitral cell (MC) somata were patched using 1–2 MΩ borosilicate glass pipettes; granule cell (GC) somata were patched using 5–7 MΩ pipettes. Membrane voltage was clamped at −70 mV. In all recordings, a 200 μs biphasic stimulus was delivered through a glass monopolar electrode placed in the external plexiform layer (EPL) within 50 μm of the mitral cell layer (MCL). For mitral cell recordings the stimulus electrode was placed 200–300 μm away, along the MCL, from the mitral cell being recorded. For granule cell recordings, the stimulus electrode was placed just above the MCL at the point nearest to the granule cell being recorded. The stimulus was varied from 1 to 50 μA and the stimulus electrode moved within about 100 μm until the synaptic response was maximized, up to 500 pA in granule cell and 1 nA in mitral cells. Most experiments were performed at room temperature, 19–22°C, except for those noted to have been performed at 35°C.

For whole-cell granule cell recordings, a potassium gluconate-based internal solution was used (mM: 136 potassium gluconate, 10 NaCl, 20 Hepes, 2 $MgSO_4$, 3 Na_2ATP, 0.2 Na_3GTP, 0.2 EGTA, pH 7.3, osmolality 290–300 mosmol kg^{-1}). For whole-cell mitral cell recordings in which an inward chloride current was preferable, a mixed potassium chloride and potassium gluconate internal solution was used (mM: 68 KCl, 68 potassium gluconate, 10 Hepes, 2 $MgSO_4$, 3 Na_2ATP,

0.2 Na_3GTP, 0.2 EGTA, pH 7.3, osmolality 290–300 mosmol kg^{-1}). In some experiments, 100 μM APV and 5 μM CNQX were added to the bath to isolate inhibitory currents. In some other experiments, 50 μM bicuculline or 50–100 μM picrotoxin was added to the bath to isolate excitatory currents. In some experiments 1 μM TTX was added to the bath to block voltage-gated sodium currents.

Imaging

Mitral or granule cells were recorded with pipette solutions containing 30–50 μM Alexa-488 or Alexa-594 (Molecular Probes, Eugene, OR, USA). Image stacks (Z steps of 1.5–2.5 μm, 16–36 steps) were obtained using a confocal microscope (Olympus Fluoview attached to a BX50WI, 40×, 0.8 NA water immersion objective, Olympus, Melville, NY, USA) with appropriate filter sets.

Data analysis

Currents were analysed using custom routines in MATLAB. The peak amplitude of the synaptic current was defined as the average of a 0.5 ms window centred on the peak. If a current was evoked before the previous current had returned to baseline, an average of currents recorded in that cell was scaled to match the previous current, and used to estimate the residual current still present at the time of the second peak. This estimated residual current was subtracted from the recorded second peak. Miniature currents were analysed using the commercially available MiniAnalysis program (Synaptosoft, Decatur, GA, USA), with a threshold set to 3 times the RMS noise. The rise time of a current was defined as the time it took for a current to increase from 10% of its maximum amplitude to 90% of its maximum. The decay time was defined as the time to decrease from 90% to 37% maximum amplitude. Dendrodendiritic inhibition was measured by integrating a 280 ms period after the cessation of stimulation. Student's *t* test was used to determine statistical significance. All errors are expressed as the standard error of the mean.

Results

Dendrodendritic inhibition displays short-term plasticity

We first confirmed that dendrodendritic inhibition (DDI) could be triggered by depolarization of mitral cells in voltage clamp, in the presence of TTX and normal extracellular Mg^{2+} (Fig. 1*B*, top). When exposed to odours, mitral cells typically fire bursts of one to five action potentials at the crest of subthreshold oscillations that follow respiriation at about 2 Hz (Imamura *et al.* 1992; Yokoi *et al.* 1995; Luo & Katz, 2001; Cang & Isaacson, 2003). We stimulated DDI using bursts of brief (1–5 ms) voltage steps in normal Mg^{2+}. The degree of recurrent inhibition evoked by a burst of short voltage steps was reliably depressed by a previous burst (Fig. 1*B*, bottom). After two trains of 5 ms voltage steps to 0 mV at 100 Hz, the

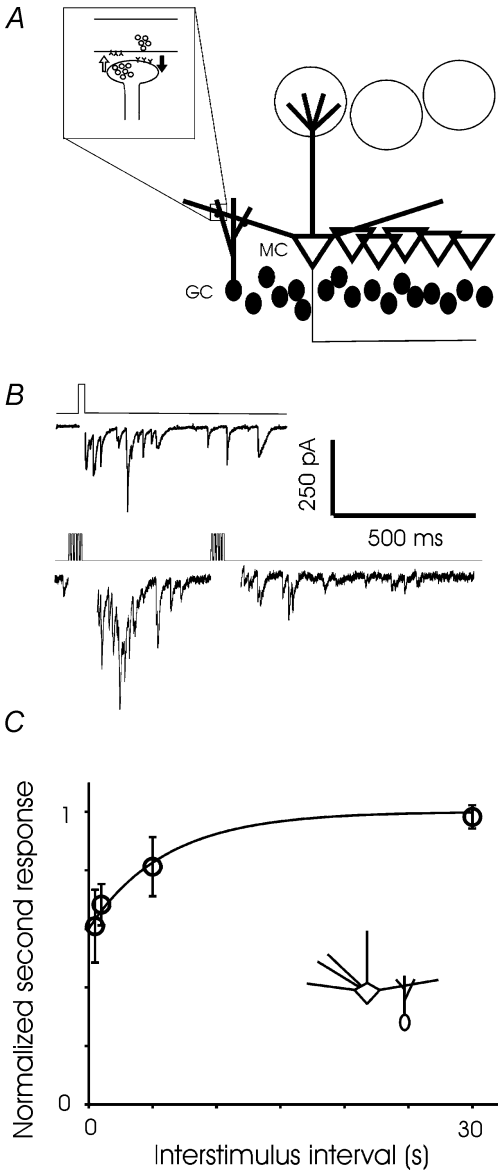

Figure 1. The mitral-granule reciprocal synapse
A, schematic diagram of the mitral–granule reciprocal synapse. *B*, an example of asynchronous IPSCs evoked in a mitral cell by a 25 ms depolarization in the presence of TTX and 1.5 mM extracellular magnesium (top). In the bottom panel, recording in 1.5 mM magnesium but no TTX, a brief train of depolarizing steps (1 ms × 5, 100 Hz) repeated at 500 ms intervals reveals depression of DDI. *C*, paired-pulse modulation of DDI. DDI was evoked with 100-Hz bursts of 5 or 10 5-ms voltage steps to 0 mV in the presence of 1.5 mM magnesium. Two bursts were applied at interstimulus intervals ranging from 500 ms to 30 s ($n = 3$ cells for the 500 ms, 1 s, and 30 s intervals; $n = 4$ for the 5 s interval).

second DDI current was depressed to 60.9 ± 12% of the first after an interval of 500 ms (Fig. 1*C*). The depression recovered with a time constant of about 6 s, such that full recovery occurred within 30 s. In the rest of this study, we investigated short-term plasticity at each side of the mitral–granule cell reciprocal synapse.

Evoked and spontaneous synaptic responses in mitral cells

We first studied the granule-to-mitral (GC-to-MC) inhibitory synapse in isolation. Recording from a mitral cell and stimulating in the external plexiform layer (EPL) in the presence of glutamate blockers (CNQX, 5 μM, and APV, 100 μM), we evoked synaptic currents of several hundred picoamps (Fig. 2*A*). Mitral cells receive GABAergic synapses both from granule cells in the EPL and from periglomerular cells in the glomerular layer. Mitral–granule reciprocal synapses constitute 80% of the synapses in the external plexiform layer (Shepherd & Greer, 1998). We believe that, by stimulating very close to the mitral cell layer (several hundred micrometres from the glomerular layer), and by using brief extracellular stimuli, we minimized potential contribution to the observed current by periglomerular cells. The synaptic currents were abolished by antagonists of $GABA_A$ receptors (Fig. 1*D*). TTX reversibly blocked the evoked current (data not shown), indicating that the responses were caused by action potential-evoked release.

To compare the evoked response with spontaneous events, we recorded spontaneous inhibitory postsynaptic currents (sIPSC) in the presence of tetrodotoxin (TTX) (Fig. 2*C*). The average frequency of these TTX-insensitive events was 0.91 ± 0.16 Hz, with an average amplitude of 60.3 ± 4.7 pA, a rise time of 4.1 ± 0.2 ms, and a decay time of 16.2 ± 0.6 ms ($n = 9$ cells). Evoked IPSCs had an average rise time of 4.6 ± 0.4 ms, a decay time of 15.3 ± 0.6 ms and amplitude of 242.0 ± 22.3 pA ($n = 8$ cells). The close kinetic similarity of evoked responses and sIPSCs (Fig. 1*D*), and the short delay between

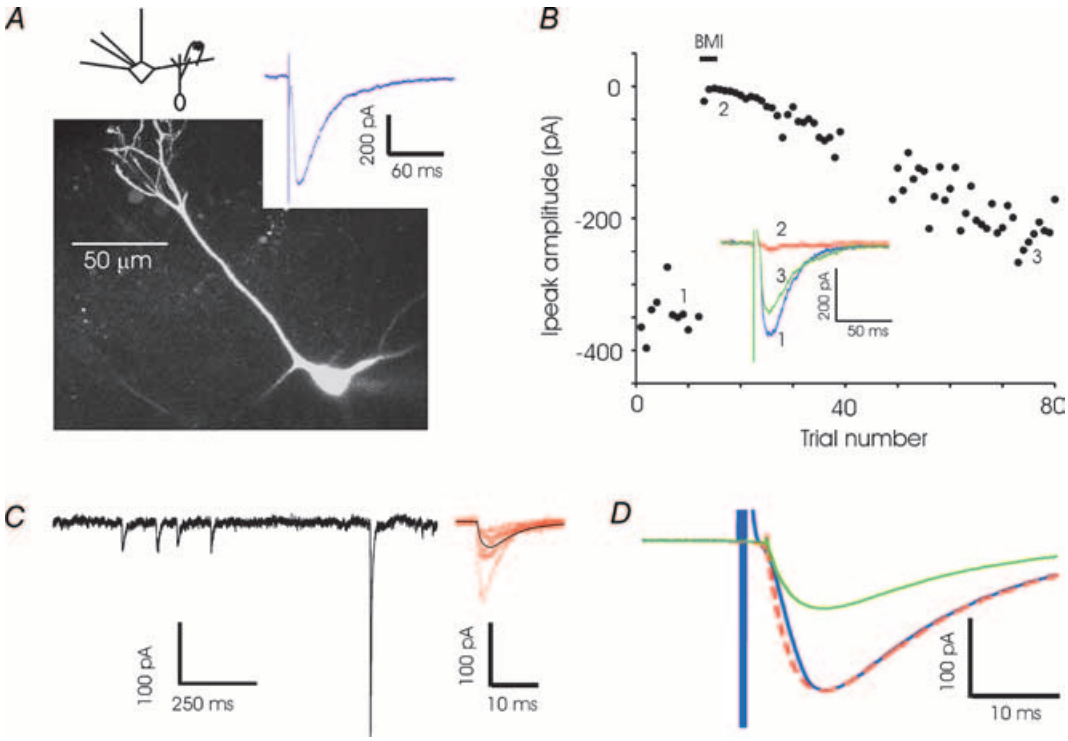

Figure 2. GC-to-MC recordings
A, an example of a whole-cell recording from a mitral cell (MC) and an image of an MC that was filled with Alexa-488 dye and imaged with a confocal microscope. Synaptic currents were recorded by stimulating extracellularly in the EPL (200 μs, 4 μA) in the presence of CNQX (5 μM) and APV (100 μM). The lateral dendrites are truncated in this image and the pipette is visible (out of focus) at the base of the cell. *B*, bicuculline (BMI, 50 μM) reversibly abolishes the evoked current (points 35-50 were distorted by an artifact and have been blanked). *C*, examples of spontaneous inhibitory postsynaptic currents recorded in the presence of TTX and glutamate blockers in a single mitral cell. Sample events at higher resolution (red) and the average of 90 events (black) are shown at right. *D*, average spontaneous IPSC ($n = 9$ cells) and evoked IPSC ($n = 8$ cells) recorded in the presence of glutamate blockers illustrates the similarity of the kinetics. The average spontaneous IPSC is also shown scaled to the peak of the average evoked IPSC (dashed line).

stimulus and response strongly suggest that the evoked responses were monosynaptic. Spontaneous events may be multivesicular, since very large events, up to 1 nA in amplitude, were observed in the presence of TTX. Presumably, the GC-to-MC synapse can release multiple vesicles in a coordinated manner even in the absence of sodium action potentials, possibly due to release of calcium from internal stores in the granule cell spine, as previously described for axonal release sites in the cerebellum (Llano *et al.* 2000), or by the opening of T-type calcium channels (Egger *et al.* 2003). We also note that, although asynchronous release could be readily evoked by sustained depolarization of mitral cells in the presence of magnesium and TTX (Fig. 1*B*), the synaptic currents evoked by EPL stimulation were brief.

Evoked and spontaneous synaptic responses in granule cells

We next isolated the mitral-to-granule (MC-to-GC) excitatory synapse by making whole-cell voltage clamp recordings from granule cells. EPL stimulation yielded synaptic currents with peak amplitudes of a few hundred picoamps (Fig. 3*A*). To ensure that we were recording solely from GCs and not from any other cell type (for example, short axon cells) that might be present in the granule cell layer, we filled a number of putative GCs with Alexa-594 dye. Nearly all cells had spiny morphologies with no detectable axons, and had large input resistances and low membrane capacitance. The few putative short-axon cells filled with dye (2 out of 37) had high capacitance

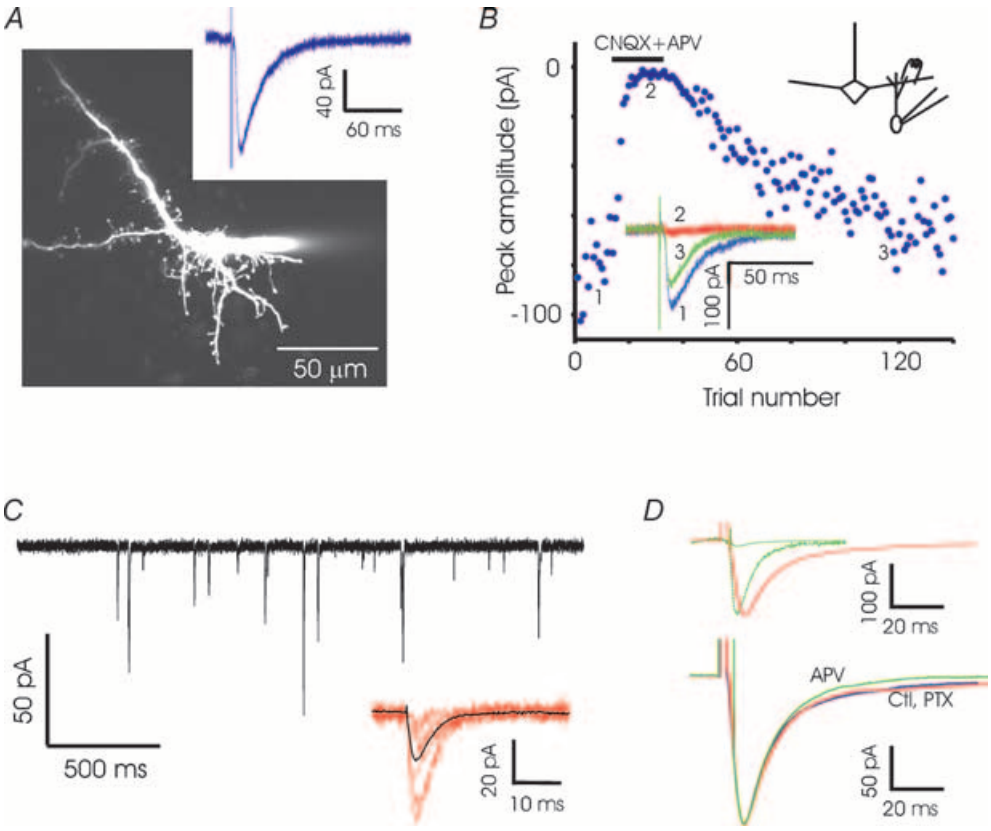

Figure 3. MC-to-GC recordings
A, fluorescence image of a granule cell (GC) filled with Alexa-594 showing abundant spines. The patch pipette is visible to the right of the cell body. A sample trace recorded in a GC shows the excitatory currents evoked by EPL stimulation (200 μs, 20 μA). *B*, the evoked current is reversibly abolished by glutamate blockers APV (100 μM) and CNQX (5 μM) (black bar). *C*, individual mEPSCs recorded in a granule cell in the presence of TTX and picrotoxin. Sample events at higher resolution (red) and the average of 100 events (black) are shown below. *D*, top, the average mEPSC from 13 granule cells and the average evoked EPSC from 9 cells are superimposed. Scaling up the mEPSC (dashed line) to match the evoked current reveals the slower decay of the evoked current. Bottom, average evoked synaptic currents recorded in control conditions (Ctl, $n = 9$), in the presence of picrotoxin (PTX, $n = 14$) and in the presence of APV ($n = 7$).

(> 100 pF) and did not respond to EPL stimulation; any cells not responding to EPL stimulation were automatically excluded from our study.

Spontaneous excitatory postsynaptic currents (sEPSCs) recorded in the presence of TTX and picrotoxin had an average frequency of 2.9 ± 1.1 Hz, with a rise time of 2.2 ± 0.4 ms, decay time of 5.8 ± 0.8 ms and average amplitude of 14.1 ± 1.2 pA ($n = 13$). Evoked EPSCs (average amplitude 190.7 ± 31.1 pA, $n = 9$) were significantly larger than sEPSCs, suggesting that the extracellular stimulation we used recruited multiple synapses (Fig. 3*C* and *D*). The rise time and decay time of evoked responses were 2.8 ± 0.4 ms and 16.9 ± 2.9 ms, respectively; the decay time was significantly larger than that of mEPSCs or spontaneous events. The kinetics of the evoked EPSC were unchanged by the addition of the $GABA_A$ receptor antagonist picrotoxin. Although we described the decay of the evoked EPSC with a single exponential for convenience, there was an additional small slow component (< 10% contribution). Only a part of this slow current was abolished by APV (Fig. 3*D*). Examination of individual traces of granule cell responses revealed occasional delayed EPSCs which might contribute to the slow decay of evoked currents (data not shown).

We also examined possible non-glutamatergic contributions to the observed current. GABAergic currents have been reported in granule cells (Carleton *et al.* 2003). We could evoke small bicuculline-sensitive currents in granule cells with EPL stimulation, provided we used an internal solution with high chloride concentration that provided a larger driving force at −70 mV (data not shown). In our regular experiments using an internal solution designed to minimize chloride currents, however, we found no change in the currents upon application of picrotoxin, and no difference in the paired-pulse modulation of the currents recorded in the presence of picrotoxin (online Supplemental material, Supplemental Fig. 1). Most of our granule cell recordings were made in the absence of $GABA_A$ receptor antagonists, whose presence increased spontaneous activity in the slice and interfered with evoked currents.

Short-term plasticity

The degree of modulation induced in a synapse by recent activity is determined by the interval since the last event, the cumulative effect of all recent events, and the amount of recovery from previous modulation. In order to study these three factors in relative isolation, we chose three stimulus patterns that cover much of the range of firing patterns observed *in vivo*. First, we examined the response to pairs of stimuli, which allowed us to vary the interpulse interval widely. To examine the effect of cumulative modulation, we used trains of 10 stimuli at 10–40 Hz, 10 being enough to yield a steady-state response. In order to examine recovery from complete depression, we used a six-pulse, 100 Hz stimulus, which reliably reduced the response to nearly zero. In all three stimulus patterns, individual trials were separated by an intertrial interval sufficient for the initial response to recover to its baseline level; for paired-pulse experiments, the intertrial interval was 30 s, and for 10–40 Hz and 100 Hz trains, 60 s.

Paired-pulse modulation

We first delivered paired stimuli separated by different interpulse intervals. The GC-to-MC inhibitory synapse was characterized by consistent and marked paired-pulse depression over intervals of 25 ms to 10 s; this depression recovered fully within 30 s (Fig. 4). In contrast, the MC-to-GC excitatory synapse displayed considerable heterogeneity in paired-pulse modulation, covering a range of depression and facilitation (Fig. 4*D*). Within an individual cell, the level of facilitation or depression was consistent from trial to trial, but between cells the level of modulation varied considerably. The MC-to-GC currents recorded in each cell could be separated into largely facilitating and largely depressing currents, based on their value at the 100 ms interval (Fig. 4). On average, the excitatory synapses onto granule cells exhibited slight depression at 25 ms intervals and slight facilitation at longer intervals, ultimately recovering completely within 500 ms. The heterogeneity in response was not readily correlated with passive properties of the neurone such as input resistance or capacitance, or with the general morphology of the neurone (Supplemental Fig. 2). Currents recorded in granule cells, both spontaneous and stimulus-evoked, also displayed quite variable kinetics. Interestingly, across different granule cells the kinetics of the evoked events were strongly correlated with those of the spontaneous events (data not shown). Although the series resistance is expected to contribute to some filtering of fast events, we found no correlation between the series resistance and the time course of evoked and spontaneous currents across different cells (Supplemental Fig. 2).

Steady state depression during trains of stimuli

Stabilization at a steady state of depression during trains has been observed at many other synapses (Markram & Tsodyks, 1996; Varela *et al.* 1997; Hempel *et al.* 2000). To study the steady state depression at the two sides of the reciprocal synapse, we recorded responses to brief trains of stimuli (Fig. 5). During 10 Hz trains, the GC-to-MC inhibitory current depressed within 150 ms and stabilized at a steady state of $24.6 \pm 0.1\%$ of the initial value (Fig. 5*C*). During 20 Hz trains the steady state value was $22.2 \pm 0.01\%$, and during 40 Hz trains, $22.4 \pm 0.1\%$ (Fig. 5*C*). The steady states at the three

stimulus frequencies were not significantly different (Student's t test, pairwise comparison, $P > 0.75$ for all pairs).

The MC-to-GC excitatory current again revealed a wide range of responses from facilitating to depressing (Fig. 5*F*). The MC-to-GC currents also stabilized within 150 ms and, when all cells were combined, the currents were depressed, the average steady state value becoming more depressed with increasing frequency (Fig. 5*C*). The MC-to-GC currents could also be split into facilitating or depressing groups based on the average of the second and third responses (Fig. 5*F*). At 10 Hz stimulation, 4 of 14 cells were facilitating; at 20 Hz, 6 of 19, and at 40 Hz, only 1 of 14. These ratios of facilitating to depressing cells correspond nicely to the number of granule cells that display paired-pulse facilitation at the 100 ms, 50 ms and 25 ms intervals, respectively. The steady state value of depressing cells was 52.7 ± 2.8% at 10 Hz, 36.5 ± 3.0% at 20 Hz, and 30.1 ± 4.7% at 40 Hz; the 10 Hz value is highly significantly different ($P < 0.001$) from both 20 and 40 Hz, while 20 and 40 Hz are not significantly different from one another. The steady state value of facilitating cells was 99.4 ± 9.3%

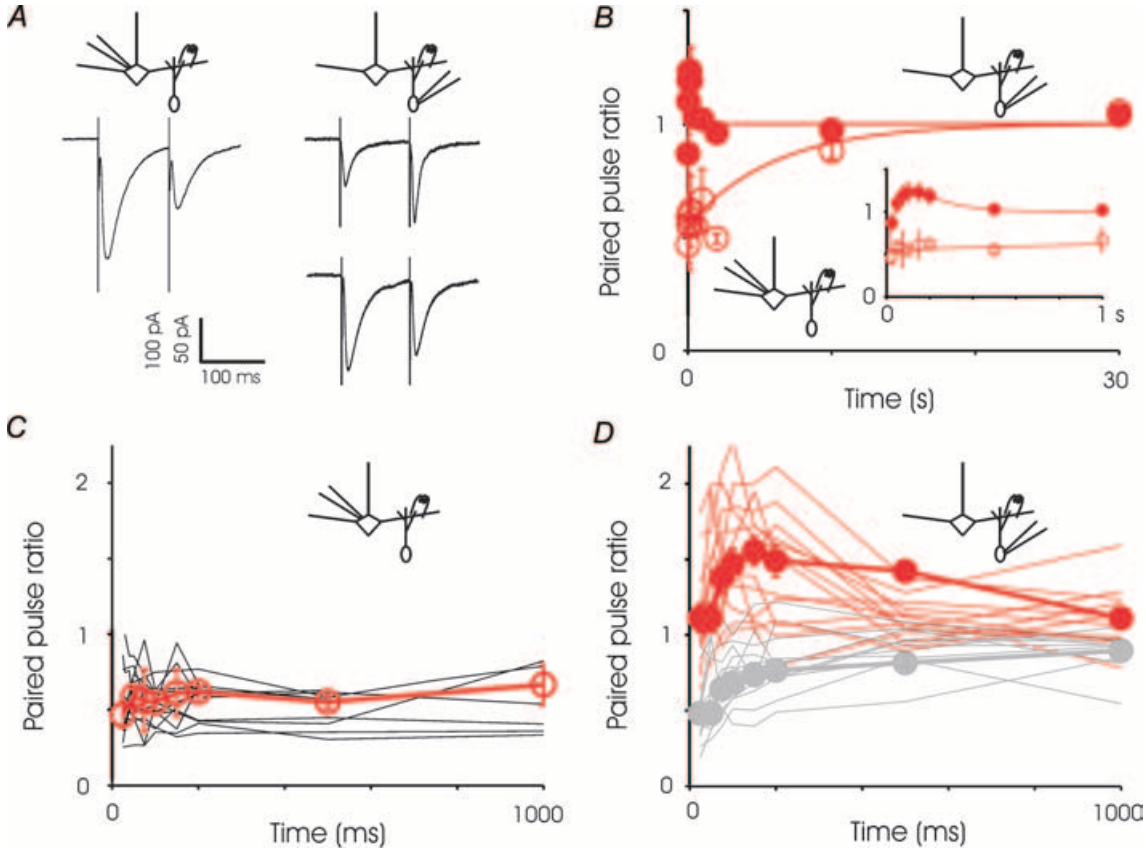

Figure 4. Paired-pulse modulation
A, right, sample recordings from a mitral cell showing paired-pulse depression at 100 ms interval (average of 16 trials). Left, sample recordings from two granule cells, one showing facilitation at 100 ms interval (average of 13 trials) and one showing depression at this same interstimulus interval (average of 16 trials). *B*, summary of paired pulse experiments for the two sides of reciprocal synapse showing an average of all cells. The GC-to-MC synapse exhibits marked paired-pulse depression at all intervals examined and the data could be described by a single exponential with a time constant of about 6 s. In contrast, the MC-to-GC synapse shows a combination of depression and facilitation. The fitted line is a sum of two exponentials – one for depression with a time constant of 45 ms and one for facilitation with a time constant of 150 ms. Icons indicate the direction of the synapse studied. For GC-to-MC synapses, each point represents 6–14 cells; for MC-to-GC synapses, reach point represents 7–24 cells. Inset, a close-up of intervals up to 1 s, showing the region of greatest contrast between the two sides of the synapse. Up to intervals of 1 s, for each time point, the data for MC are different from GC at $P < 0.05$. *C*, traces showing the recording of the GC-to-MC current at various interpulse intervals in individual mitral cells. The average of all cells is superimposed. *D*, traces showing the recording of the MC-to-GC current at various interpulse intervals in individual granule cells. The average of facilitating cells is superimposed in red, and of depressing cells in light grey.

at 10 Hz and 102.2 ± 8.8% at 20 Hz; these values are not significantly different from one another (Student's *t* test, $P = 0.84$). When the facilitating and depressing granule cells are combined, the 10, 20 and 40 Hz steady state values are 0.66 ± 0.07%, 0.57 ± 0.08% and 0.33 ± 0.05%, respectively (Fig. 5*D*); 40 Hz is significantly different from 20 Hz ($P < 0.05$) and highly significantly different from 10 Hz ($P < 0.01$). The GC-to-MC steady state value was relatively insensitive to increases in frequency above 10 Hz, while the MC-to-GC steady state became more likely to show depression over facilitation, and more strongly depressed when it did display depression, as the stimulus rate increased (Fig. 5*C* and *D*). These results suggest that during increases in mitral cell firing rates above 10 Hz, the

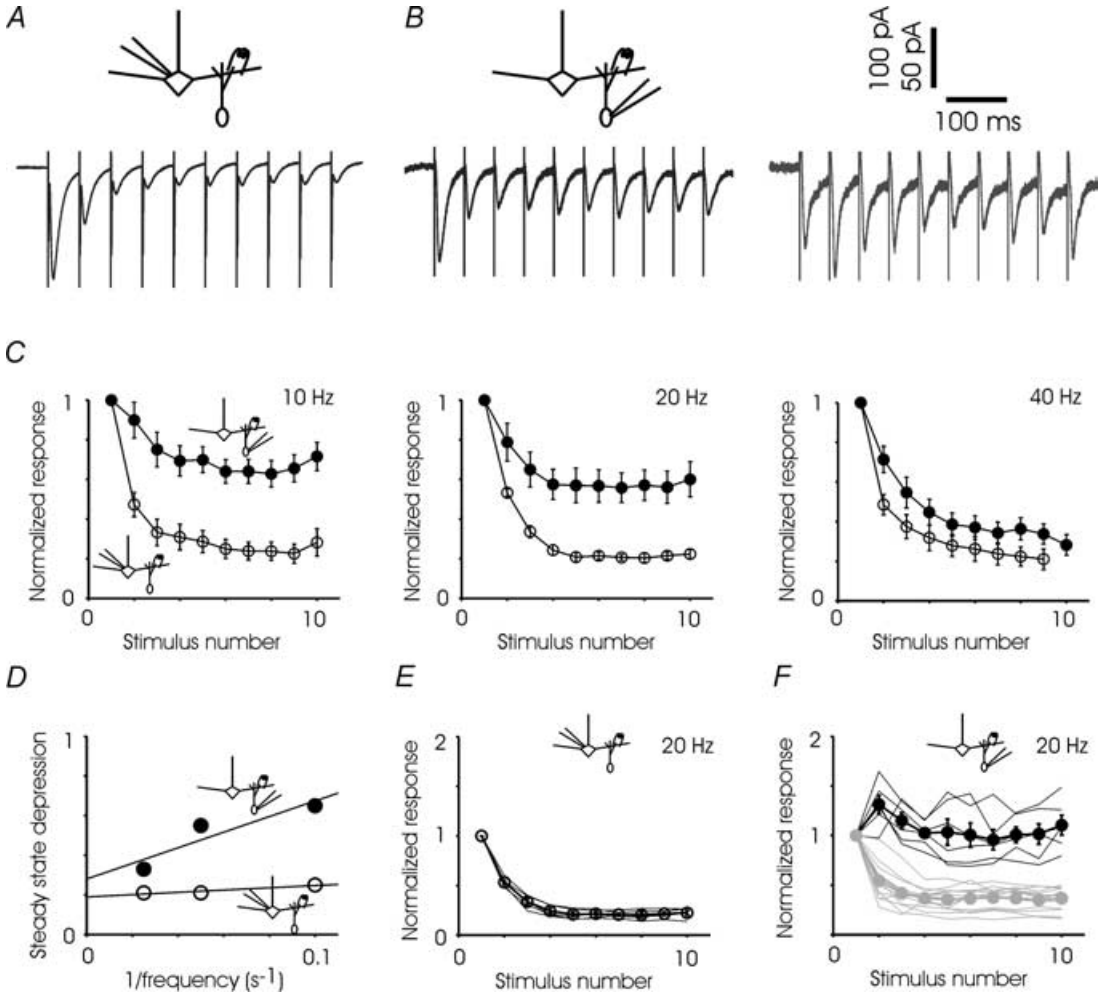

Figure 5. Responses to stimulus trains
A, sample average GC-to-MC synaptic response to 20 Hz stimulation; response is depressed to 20% of original within three pulses and remains stable for the next six. *B*, sample average MC-to-GC traces showing progressive depression in one cell and an initial facilitation followed by depression in another cell. *C*, summary of all experiments indicates substantially less depression in the MC-to-GC synapse when compared to GC-to-MC synapse at lower, but not higher, stimulus frequencies. All sets of data are fitted with single exponentials (τ of around 1 stimulus). 10 Hz: GC-to-MC $n = 14$ cells, MC-to-GC $n = 9$ cells, highly significantly different at stimulus numbers 2 through 10; 20 Hz: GC-to-MC $n = 5$, MC-to-GC $n = 19$, significantly different at stimulus numbers 4 through 10; 40 Hz, GC-to-MC $n = 8$, MC-to-GC $n = 14$, significantly different at stimulus number 2 only (Student's *t* test, significant $P < 0.05$, highly significant $P < 0.01$). *D*, steady state value of MC-to-GC and GC-to-MC currents are plotted as a function of the inverse of the stimulus frequency ($1/f$). Best-fitting straight lines are also shown. *E*, responses of the GC-to-MC currents during 20 Hz stimulation are relatively homogeneous. Individual mitral cells are shown by continuous lines and the average of all cells is shown by circles. *F*, responses of the MC-to-GC excitatory currents during 20 Hz are heterogeneous. Individual granule cell responses are shown by the continuous lines, with depressing cells in light grey. The averages of facilitating and depressing cells are also shown separately. Facilitating cells are significantly different from depressing cells at stimulus numbers 2 through 10 (Student's *t* test, $P < 0.05$).

MC-to-GC side of the synapse would be the source of most of the plasticity of the total reciprocal synapse.

Recovery from depression

Mitral cells typically fire action potentials in cycles that are phase-locked with respiration, emitting brief bursts of action potentials followed by pauses. Therefore, we characterized the time course of recovery of synaptic transmission after bursts of stimuli. A test pulse was followed by a stimulus of six shocks delivered at 100 Hz; a second, single test pulse followed the train by an interval ranging from 25 ms to 1.5 s (Fig. 6). The GC-to-MC synapse was almost completely depressed immediately after the train, and took several seconds to recover completely. The behaviour of the MC-to-GC synapse was more complex. Following a train of stimuli, the synapse was depressed at short intervals, but recovered quickly within about 300 ms and exhibited increased synaptic strength resulting from facilitation or post-tetanic potentiation. Unlike paired-pulse modulation and response to 10–40 Hz trains, recovery from depression did not reveal great heterogeneity in the MC-to-GC current; all cells recorded displayed very similar responses, and all data are pooled in the figure.

Effects of elevated calcium on paired-pulse modulation and recovery from depression

We investigated some of the mechanisms of short-term plasticity at the two sides of the synapse. At other synapses of the central nervous system, paired-pulse depression is thought to result partly from depletion of the readily releasable vesicle pool, this depletion being enhanced by high extracellular calcium (Betz, 1970; Kusano & Landau, 1975; Zucker & Regehr, 2002). We examined the changes in paired pulse modulation in elevated extracellular calcium, 5 mM compared to 2.5 mM (Fig. 7). As at other depressing synapses in the brain, high calcium increased the amplitude of all evoked responses and increased the contribution of depression at the reciprocal synapse. At both the MC-to-GC and GC-to-MC synapses, only depressing currents were observed in paired-pulse recordings in elevated extracellular calcium. A higher concentration of calcium can have complex effects at synapses. It can increase depression by enhancing initial neurotransmitter release, increase facilitation by increasing residual calcium, or decrease facilitation by saturating the release mechanism (Zucker & Regehr, 2002). At the mitral-to-granule synapse, in which depression and facilitation are both present, increased depression won out over facilitation in high calcium. Since paired-pulse modulation at the reciprocal synapse is calcium dependent, it is at least partly due to changes in presynaptic properties. Reducing extracellular calcium from 2.5 to 1.8 mM, however, had no significant effect on paired-pulse modulation at either synapse (data not shown). It is likely that the reduction from 2.5 to 1.8 was too small to reveal a major change in the level of facilitation *versus* depression. Experiments at lower calcium concentrations were attempted, but the initial release probability was sufficiently reduced as to preclude detailed characterization.

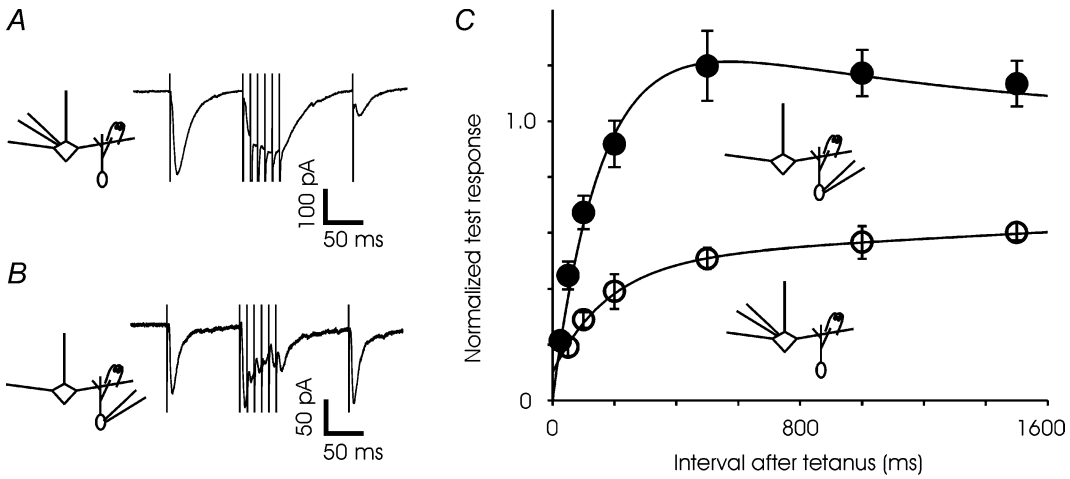

Figure 6. Different time course of recovery from depression at the two sides of the reciprocal synapse
A, synaptic currents recorded in a mitral cell in response to a single stimulus followed by 6 stimuli at 100 Hz and finally a test pulse at a variable interval (100 ms, in the trace shown) after the cessation of train (average of 12 trials). *B*, synaptic response to a similar stimulus in a granule cell (average of 5 trials). *C*, summary of all experiments indicates a dramatic difference in the recovery time course between the two sides of the synapse. The fitted curve for GC-to-MC synapse has two time constants – about 160 ms for recovery from depression and 1000 ms for facilitation. For the MC-to-GC curve, two time constants for depression (180 and 7000 ms) were used. For each time point, the data for MC are different from GC at $P < 0.05$. For GC-to-MC synapse, N = 4 cells and for MC-to-GC synapse, N = 18 cells.

We also tested the recovery of the synapses from high-frequency trains in high extracellular calcium. Recovery from depression is associated with replenishment of the vesicle pool or with mobilization of previously reluctant vesicles, and recovery is frequently calcium dependent (Kusano & Landau, 1975; Wang & Kaczmarek, 1998; Dittman & Regehr, 1998; Stevens & Wesseling, 1998). At the mitral-granule synapse, recovery from depression was not significantly affected by elevated extracellular calcium at either side of the synapse. It is possible that any effect of calcium on recovery was maximal at 2.5 mM and further increase in extracellular calcium concentration had no additional effect.

Short-term plasticity at physiological temperature and extracellular calcium concentration

To confirm our central finding, the opposing short-term plasticity of the two sides of the synapse, in conditions better approximating the physiological state, we repeated the paired-pulse modulation experiments in 1.8 mM extracellular calcium and 35°C (Fig. 8). At both sides of the synapse the observed plasticity was unchanged. The kinetics of evoked synaptic currents were, however, more rapid at higher temperatures. In MCs at 35°C, the rise time of the evoked current was 2.1 ± 0.1 ms, and the decay time 6.7 ± 0.3 ms. In GCs at 35°C, the rise time was 1.7 ± 0.1 ms, and the decay 5.5 ± 0.5 ms. All of these

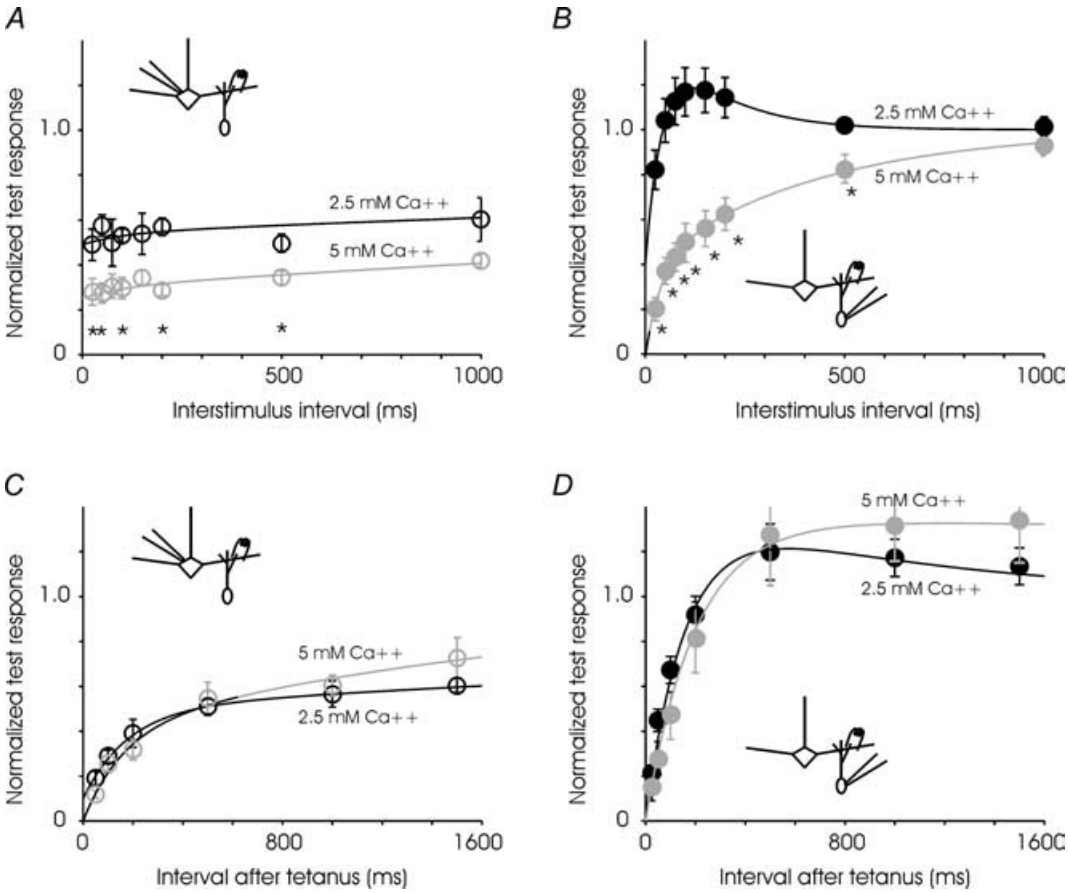

Figure 7. Calcium dependence of short-term plasticities
A, paired-pulse depression of granule-to-mitral synapse in greater in high extracellular calcium (5 mM) compared to control conditions (2.5 mM). The time constant of recovery is not significantly different in the two cases. $n = 6$–14 cells for control, and 7 cells for high calcium. Data were fitted to the expression: $1 - 0.05e^{-t/100} - 0.46e^{-t/6000}$ and $1 - 0.05e^{-t/180} - 0.7e^{-t/6000}$ for low and high calcium, respectively. *B*, at higher calcium concentration, the mitral-to-granule synapse exhibits paired-pulse depression at all intervals tested. $n = 6$–12 cells for control and 7 cells for high calcium. Data were fitted to the expression: $1 - 1.2e^{-t/45} + 0.6e^{-t/150}$ and $1 - 0.4e^{-t/40} - 0.6e^{-t/430}$ for low and high calcium, respectively. *C*, recovery from depression induced by fast trains was not substantially different at the granule-to-mtiral synapse in control (2.5 mM) and high (5 mM) calcium ($n = 4$ cells for each condition). Data were fitted to the expression: $1 - 0.4e^{-t/180} - 0.5e^{-t/7000}$ and $1 - 0.4e^{-t/160} - 0.6e^{-t/2000}$ for low and high calcium, respectively. *D*, recovery from depression at the mitral-to-granule synapse was also not affected significantly by increased extracellular calcium. (Control, $n = 4$ cells, high calcium, $n = 5$ cells.) Data were fitted to the expression: $1 - 1.45e^{-t/160} + 0.45e^{-t/1000}$ and $1 - 1.35e^{-t/200} + 0.35e^{-t/20000}$ for low and high calcium, respectively. Asterisks denote time points at which pair-wise comparisons within each panel reveals a difference at $P < 0.05$.

rise and decay times were significantly different from their room-temperature counterparts ($P < 0.01$).

Discussion

Short-term synaptic plasticity has been linked to information processing in many sensory regions of the brain (Markram & Tsodyks, 1996; Abbott *et al.* 1997; Cook *et al.* 2003). In the olfactory system, odour information is thought to be processed and transformed within the olfactory bulb before it is transmitted downstream to cortical areas (Shipley & Ennis, 1996; Laurent, 1999; Mori *et al.* 1999; Schoppa & Urban, 2003). The dendrodendritic synapses between mitral and granule cells are ideally situated to permit cross flow of information between multiple glomeruli in the olfactory bulb. In particular, dynamic changes in synaptic strength at the reciprocal synapse on a subsecond time scale could shape the responses of mitral cells to time-varying stimuli. Here, we examined short-term dynamics of the two sides of the reciprocal synapse and have discovered interesting differences between them that may have important consequences for olfactory information processing. The major finding of our study is that short-term plasticity at inhibitory synapses on mitral cell dendrites is significantly different from that of excitatory synapses on granule cells. The MC-to-GC excitatory synapse is rather stable during repetitive stimulus, maintaining its efficacy and recovering quickly during brief pauses of half a second or less. In contrast, the GC-to-MC inhibitory synapse depresses quickly and recovers slowly from depression. The short-term dynamics of the autoinihibitory circuit (Fig. 1*B*) appears to be dominated by the recovery of the granule-to-mitral synapse.

Time course of GABAergic currents in mitral cells

In our study, we evoke GABA release with brief extracellular stimuli in the presence of physiological levels of magnesium. This contrasts with most studies of reciprocal and lateral inhibition where GABA release is evoked by prolonged depolarization of a mitral cell (Chen & Shepherd, 1997; Isaacson & Strowbridge, 1998; Friedman & Strowbridge, 2000; Margrie *et al.* 2001) or enhanced by reducing extracellular magnesium (Schoppa *et al.* 1998; Chen *et al.* 2000; Halabisky *et al.* 2000). Other studies have anecdotally reported extracellular stimuli that yield fast, smooth summated currents like those we study here (Schoppa & Westbrook, 1999; Chen *et al.* 2000; Isaacson & Vitten, 2003). It is unclear from previous studies whether the extended time course of dendrodendritic inhibition reflects multiple release events from a single granule cell, or asynchronous release from a large number of granule cells. In the glomerular dendrodendritic circuit, a single tufted cell can excite many periglomerular interneurones, which fire at variable times following tufted cell activation (Murphy *et al.* 2005). Future experiments will be required to determine whether a similar pattern

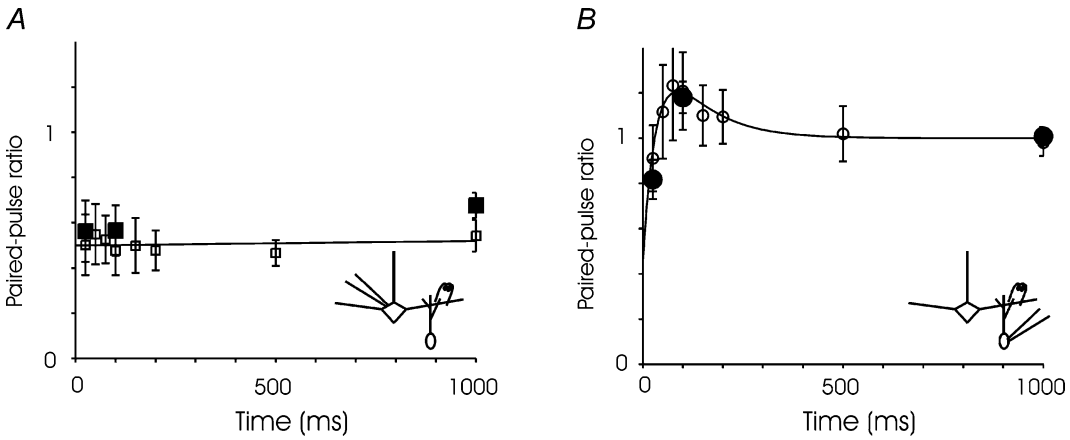

Figure 8. Paired pulse modulation in physiological conditions
A, in 1.8 mM extracellular calcium, the modulation of the GC-to-MC synapse is unchanged from that measured at 2.5 mM calcium, exhibiting marked paired-pulse depression at all intervals examined (□). The data could be described by a nearly flat line (or a single exponential with a very long time constant). At three interstimulus intervals (25, 100 and 1000 ms), the level of depression is unchanged at 1.8 mM calcium and 35°C (■). At all intervals and temperatures, the level of depression is not statistically significantly different from levels measured in 2.5 mM calcium. *B*, in 1.8 mM calcium (○), the modulation of the MC-to-GC synapse shows a combination of depression and facilitation unchanged from that measured at 2.5 mM calcium, and the effect is unaltered at 35°C (●). The fitted line is a sum of two exponentials – one for depression has a time constant of 35 ms and one for facilitation 100 ms. For GC-to-MC synapses, $n = 6$ at room temperature and 6 at 35°C, and for MC-to-GC synapses, $n = 13$ at room temperature and 10–16 at 35°C.

of activation occurs in the mitral–granule cell circuit. We occasionally see asynchronous release following our brief stimulus pulse, but the release, when present, is much smaller in amplitude than the coordinated release immediately following the stimulus. The total current contributed by asynchronous events in a 1.5-s period following stimulus (after baseline subtraction) was less than 2% of the evoked current. We conclude that, after a single action potential, the bulk of granule cell release onto mitral cells is quite brief.

Heterogeneity of MC-to-GC currents

We observed that MC-to-GC excitatory currents recorded in granule cells vary widely in their paired-pulse modulation and steady state response to trains; some cells have currents that primarily facilitate, while others primarily depress. A particular cell displays consistent facilitation or depression across different interpulse intervals, and the levels of facilitation and depression are not obviously correlated with intrinsic cell properties or with gross measures of morphology (Supplemental Fig. 2). The MC-to-GC currents stand in contrast to the GC-to-MC inhibitory currents, which are very similar from cell to cell. This source of this heterogeneity is an exciting question for further research. A first question to pursue will be to determine whether the source of the heterogeneity is primarily presynaptic, in the mitral cells that excite the granule cell in question, or postsynaptic, in the granule cell itself. Possible sources of the heterogeneity on the postsynaptic side include the type of granule cell (as defined morphologically), the receptor subtypes expressed by the cell, the types of centrifugal input received by the cell, and most intriguingly, the age of the granule cell.

Calcium dependence of short-term plasticity

We have shown above that paired-pulse modulation at the reciprocal synapse is calcium dependent, and therefore at least partly presynaptic. Increasing extracellular calcium enhances initial release and promotes paired-pulse depression, but does not significantly affect recovery from depression. A reduction in release probability for the second of a paired stimulus can be due to alteration in calcium entry, depletion of releasable vesicles or desensitization of the release machinery (Zucker & Regehr, 2002). Elucidating the precise contribution of each of these factors will require a comprehensive set of new experiments. We note, however, that the predominance of depression at the GC-to-MC synapse and of facilitation at many MC-to-GC synapses may be related to differences in the number and distribution of vesicles in granule cell spines and mitral cell dendrites (Price & Powell, 1970). Such a dependence of release properties on vesicle number has been described at some synapses (Schikorski & Stevens, 1999), but not at others (Xu-Friedman & Regehr, 2004). Further studies can also determine any role of metabotropic receptors or postsynaptic factors such as receptor desensitization in the different forms of short-term plasticity described here.

Spike-mediated versus spike-independent release

It is well known that vesicle release can occur from granule cell spines in the presence of TTX, presumably through local depolarization and calcium influx through T-type calcium channels and, possibly, NMDA receptors (Chen & Shepherd, 1997; Isaacson & Strowbridge, 1998; Schoppa *et al.* 1998; Halabisky *et al.* 2000; Isaacson, 2001; Egger *et al.* 2003). It has been proposed that granule cells can inhibit mitral cell firing in two different ways: local, in which a single spine reciprocally inhibits only the mitral cell which excited it, and global, in which the granule cell fires and inhibits all of its mitral cell partners, whether they contributed to its firing or not (Egger *et al.* 2003). In our study, we investigated only spike-mediated vesicle release from granule cells. It is of interest to know if the mechanisms we have described apply to spike-independent reciprocal inhibition.

Implications for lateral inhibition and information processing in the olfactory bulb

Mitral cells laterally inhibit one another through mitral–granule–mitral circuits. It has been demonstrated that local granule cell inhibition can block action potential propagation along the mitral cell lateral dendrites (Lowe, 2002; Xiong & Chen, 2002). During periods of relatively low mitral cell firing, propagation might be limited to the relatively proximal portions of the lateral dendrites. During periods of high firing rates, the GC-to-MC inhibitory synapses would become strongly depressed, presumably permitting action potentials to propagate and reach more distal synapses. These distal synapses, shielded from previous activity, would be in a fully recovered state and available for a new round of auto- and lateral inhibition. In particular, distinct networks of mitral cells could be linked together by proximal granule cells, which would be active during low levels of mitral cell activity but quickly depressed by fast spiking, and distal granule cells, which would be unmasked and become active only after fast spiking. This latter mechanism of dynamic gating might apply to an observation made by Urban & Sakmann (2002) – in mitral cells coupled in an inhibitory manner, the extent of depression increases from the first to the last stimulus during trains of action potentials. Such a scenario, in which successive networks of mitral–granule–mitral circuits are revealed as proximal networks are depressed by

high firing rates, is, however, only one of many possibilities suggested by our data.

Although it is generally agreed that granule cell inhibition is critical for sharpening odour representations in the olfactory bulb, consensus on the bulb's computational strategy has not been reached. Two models have been proposed: first, that similar odours are mapped close together on the bulb, and granule cells create centre-surround fields similar to those in the retina (Mori *et al.* 1999); second, that individual odours are represented as synchronously firing groups of mitral cells, and granule cells serve to synchronize these groups (Laurent, 1999). These models are not mutually exclusive, and it is possible that they are both relevant to processing in the olfactory bulb. It has been suggested that because reciprocal and lateral inhibition can last for seconds after a mitral cell is stimulated, granule-cell-mediated GABAergic currents are too slow and asynchronous to effect synchronous spiking between mitral cells (Schoppa & Urban, 2003). Our data suggest that spike-mediated release of GABA from granule cells is very brief and could allow precise patterning of mitral cell spikes, thereby allowing the reciprocal synapse to participate in both proposed models. Future models of reciprocal inhibition in the bulb could incorporate two separate temporal phases when considering single neurone interactions – a fast, coordinated release of vesicles yielding large-amplitude current, and a slow, asynchronous release yielding a small-amplitude current.

References

Abbott LF, Varela JA, Sen K & Nelson SB (1997). Synaptic depression and cortical gain control. *Science* **275**, 220–224.

Aungst JL, Heyward PM, Puche AC, Karnup SV, Hayar A, Szabo G & Shipley MT (2003). Centre-surround inhibition among olfactory bulb glomeruli. *Nature* **426**, 623–629.

Betz WJ (1970). Depression of transmitter release at the neuromuscular junction of the frog. *J Physiol* **206**, 629–644.

Cang J & Isaacson JS (2003). In vivo whole-cell recording of odor-evoked synaptic transmission in the rat olfactory bulb. *J Neurosci* **23**, 4108–4116.

Carleton A, Petreanu LT, Lansford R, Alvarez-Buylla A & Lledo PM (2003). Becoming a new neuron in the adult olfactory bulb. *Nat Neurosci* **6**, 507–518.

Chen WR & Shepherd GM (1997). Membrane and synaptic properties of mitral cells in slices of rat olfactory bulb. *Brain Res* **745**, 189–196.

Chen WR, Xiong W & Shepherd GM (2000). Analysis of relations between NMDA receptors and GABA release at olfactory bulb reciprocal synapses. *Neuron* **25**, 625–633.

Cook DL, Schwindt PC, Grande LA & Spain WJ (2003). Synaptic depression in the localization of sound. *Nature* **421**, 66–70.

DeVries SH & Baylor DA (1993). Synaptic circuitry of the retina and olfactory bulb. *Cell* **72** (Suppl.), 139–149.

Dittman JS, Kreitzer AC & Regehr WG (2000). Interplay between facilitation, depression, and residual calcium at three presynaptic terminals. *J Neurosci* **20**, 1374–1385.

Dittman JS & Regehr WG (1998). Calcium dependence and recovery kinetics of presynaptic depression at the climbing fiber to Purkinje cell synapse. *J Neurosci* **18**, 6147–6162.

Egger V, Svoboda K & Mainen ZF (2003). Mechanisms of lateral inhibition in the olfactory bulb: efficiency and modulation of spike-evoked calcium influx into granule cells. *J Neurosci* **23**, 7551–7558.

Friedman D & Strowbridge BW (2000). Functional role of NMDA autoreceptors in olfactory mitral cells. *J Neurophysiol* **84**, 39–50.

Halabisky B, Friedman D, Radojicic M & Strowbridge BW (2000). Calcium influx through NMDA receptors directly evokes GABA release in olfactory bulb granule cells. *J Neurosci* **20**, 5124–5134.

Halabisky B & Strowbridge BW (2003). Gamma-frequency excitatory input to granule cells facilitates dendrodendritic inhibition in the rat olfactory Bulb. *J Neurophysiol* **90**, 644–654.

Hamilton KA & Kauer JS (1989). Patterns of intracellular potentials in salamander mitral/tufted cells in response to odor stimulation. *J Neurophysiol* **62**, 609–625.

Hempel CM, Hartman KH, Wang XJ, Turrigiano GG & Nelson SB (2000). Multiple forms of short-term plasticity at excitatory synapses in rat medial prefrontal cortex. *J Neurophysiol* **83**, 3031–3041.

Imamura K, Mataga N & Mori K (1992). Coding of odor molecules by mitral/tufted cells in rabbit olfactory bulb. I. Aliphatic compounds. *J Neurophysiol* **68**, 1986–2002.

Isaacson JS (2001). Mechanisms governing dendritic gamma-aminobutyric acid (GABA) release in the rat olfactory bulb. *Proc Natl Acad Sci U S A* **98**, 337–342.

Isaacson JS & Strowbridge BW (1998). Olfactory reciprocal synapses: dendritic signaling in the CNS. *Neuron* **20**, 749–761.

Isaacson JS & Vitten H (2003). $GABA_B$ receptors inhibit dendrodendritic transmission in the rat olfactory bulb. *J Neurosci* **23**, 2032–2039.

Jahr CE & Nicoll RA (1982). An intracellular analysis of dendrodendritic inhibition in the turtle in vitro olfactory bulb. *J Physiol* **326**, 213–234.

Kashiwadani H, Sasaki YF, Uchida N & Mori K (1999). Synchronized oscillatory discharges of mitral/tufted cells with different molecular receptive ranges in the rabbit olfactory bulb. *J Neurophysiol* **82**, 1786–1792.

Kusano K & Landau EM (1975). Depression and recovery of transmission at the squid giant synapse. *J Physiol* **245**, 13–22.

Laurent G (1999). A systems perspective on early olfactory coding. *Science* **286**, 723–728.

Llano I, Gonzalez J, Caputo C, Lai FA, Blayney LM, Tan YP & Marty A (2000). Presynaptic calcium stores underlie large-amplitude miniature IPSCs and spontaneous calcium transients. *Nat Neurosci* **3**, 1256–1265.

Lowe G (2002). Inhibition of backpropagating action potentials in mitral cell secondary dendrites. *J Neurophysiol* **88**, 64–85.

Luo M & Katz LC (2001). Response correlation maps of neurons in the mammalian olfactory bulb. *Neuron* **32**, 1165–1179.

Margrie TW, Sakmann B & Urban NN (2001). Action potential propagation in mitral cell lateral dendrites is decremental and controls recurrent and lateral inhibition in the mammalian olfactory bulb. *Proc Natl Acad Sci U S A* **98**, 319–324.

Markram H & Tsodyks M (1996). Redistribution of synaptic efficacy between neocortical pyramidal neurons. *Nature* **382**, 807–810.

Meredith M (1986). Patterned response to odor in mammalian olfactory bulb: the influence of intensity. *J Neurophysiol* **56**, 572–597.

Mori K, Nagao H & Yoshihara Y (1999). The olfactory bulb: coding and processing of odor molecule information. *Science* **286**, 711–715.

Murphy GJ, Darcy DP & Isaacson JS (2005). Intraglomerular inhibition: signaling mechanisms of an olfactory microcircuit. *Nat Neurosci* **8**, 354–364.

Nicoll RA (1969). Inhibitory mechanisms in the rabbit olfactory bulb: dendrodendritic mechanisms. *Brain Res* **14**, 157–172.

Price JL & Powell TP (1970). The morphology of the granule cells of the olfactory bulb. *J Cell Sci* **7**, 91–123.

Rall W, Shepherd GM, Reese TS & Brightman MW (1966). Dendrodendritic synaptic pathway for inhibition in the olfactory bulb. *Exp Neurol* **14**, 44–56.

Schikorski T & Stevens CF (1999). Quantitative fine-structural analysis of olfactory cortical synapses. *Proc Natl Acad Sci U S A* **96**, 4107–4112.

Schoppa NE, Kinzie JM, Sahara Y, Segerson TP & Westbrook GL (1998). Dendrodendritic inhibition in the olfactory bulb is driven by NMDA receptors. *J Neurosci* **18**, 6790–6802.

Schoppa NE & Urban NN (2003). Dendritic processing within olfactory bulb circuits. *Trends Neurosci* **26**, 501–506.

Schoppa NE & Westbrook GL (1999). Regulation of synaptic timing in the olfactory bulb by an A-type potassium current. *Nat Neurosci* **2**, 1106–1113.

Shepherd GM & Greer CA (1998). Olfactory bulb. In *The Synaptic Organization of the Brain*, ed. Shepherd GM, pp. 159–203. Oxford University Press, New York.

Shipley MT & Ennis M (1996). Functional organization of olfactory system. *J Neurobiol* **30**, 123–176.

Stevens CF & Wesseling JF (1998). Activity-dependent modulation of the rate at which synaptic vesicles become available to undergo exocytosis. *Neuron* **21**, 415–424.

Stopfer M, Bhagavan S, Smith BH & Laurent G (1997). Impaired odour discrimination on desynchronization of odour-encoding neural assemblies. *Nature* **390**, 70–74.

Tsodyks MV & Markram H (1997). The neural code between neocortical pyramidal neurons depends on neurotransmitter release probability. *Proc Natl Acad Sci U S A* **94**, 719–723.

Urban NN & Sakmann B (2002). Reciprocal intraglomerular excitation and intra- and interglomerular lateral inhibition between mouse olfactory bulb mitral cells. *J Physiol* **542**, 355–367.

Varela JA, Sen K, Gibson J, Fost J, Abbott LF & Nelson SB (1997). A quantitative description of short-term plasticity at excitatory synapses in layer 2/3 of rat primary visual cortex. *J Neurosci* **17**, 7926–7940.

Wang LY & Kaczmarek LK (1998). High-frequency firing helps replenish the readily releasable pool of synaptic vesicles. *Nature* **394**, 384–388.

Wilson DA (2000). Comparison of odor receptive field plasticity in the rat olfactory bulb and anterior piriform cortex. *J Neurophysiol* **84**, 3036–3042.

Xiong W & Chen WR (2002). Dynamic gating of spike propagation in the mitral cell lateral dendrites. *Neuron* **34**, 115–126.

Xu-Friedman MA & Regehr WG (2004). Structural contributions to short-term synaptic plasticity. *Physiol Rev* **84**, 69–85.

Yokoi M, Mori K & Nakanishi S (1995). Refinement of odor molecule tuning by dendrodendritic synaptic inhibition in the olfactory bulb. *Proc Natl Acad Sci U S A* **92**, 3371–3375.

Zucker R & Regehr W (2002). Short-term synaptic plasticity. *Annu Rev Physiol* **64**, 355–405.

Acknowledgements

We thank Juan Burrone and William Tyler for critical discussions and comments. This work was supported by a Pew Scholars Award in the Biomedical Sciences to V.N.M. and a Ruth L. Kirschstein National Research Service Award to S.B.D. Research in V.N.M.'s laboratory was also supported by grants from the NIH, the NSF, the EJLB Foundation and the Klingenstein Fund.

Supplemental material

The online version of this paper can be accessed at:
DOI: 10.1113/jphysiol.2005.095844
http://jp.physoc.org/cgi/content/full/jphysiol.2005.095844/DC1
and contains supplemental material consisting of two figures:

Supplemental Fig. 1. Paired-pulse modulation of MC-to-GC currents is not significantly affected by picrotoxin

Supplemental Fig. 2. The level of paired pulse depression versus facilitation at the MC-to-GC synapse is not positively correlated with series reistance, input resistance, or capacitance of the granule cell recorded; nor is the series resistance correlated with the EPSC decay time constant

This material can also be found as part of the full-text HTML version available from http://www.blackwell-synergy.com